MICHIGAN STATE UNIVERSITY

CYCLOTRON LABORATORY

EXCITATION OF THE GIANT M1 RESONANCE BY INELASTIC PROTON SCATTERING AT 200 MeV

A. GALONSKY, N. ANANTARAMAN AND G.M. CRAWLEY
MICHIGAN STATE UNIVERSITY, EAST LANSING, MICHIGAN
AND
C. DJALALI, N. MARTY, M. MORLET, A. WILLIS AND J.-C. JOURDAIN
INSTITUT DE PHYSIQUE NUCLÉAIRE, ORSAY, FRANCE

JANUARY 1984

MSUCL-446

EXCITATION OF THE GIANT M1 RESONANCE BY INELASTIC PROTON SCATTERING AT 200 MEV

A. Galonsky*, N. Anantaraman* and G.M. Crawley*
Michigan State University, E. Lansing, Michigan and

C. Djalali, N. Marty, M. Morlet, A. Willis and J.-C. Jourdain
Institut de Physique Nucleaire, Orsay, France

Invited talk presented at the International Symposium on

ELECTROMAGNETIC PROPERTIES OF ATOMIC NUCLEI

— Thirty Years of Configuration Mixing and
Future Directions of Nuclear Shell Model —

November 9-12, 1983

To be published in the Proceedings by
Tokyo Institute of Technology

EXCITATION OF THE GIANT M1 RESONANCE BY INELASTIC PROTON SCATTERING AT 200 MEV

A. Galonsky*, N. Anantaraman* and G.M. Crawley*
Michigan State University, E. Lansing, Michigan and

C. Djalali, N. Marty, M. Morlet, A. Willis and J.-C. Jourdain
Institut de Physique Nucleaire, Orsay, France

Abstract

The (p,p') reaction at 200 MeV has been found to be strongly selective of ℓ=0, spin-flip transitions when the scattering angle is very small. A concentration of 1^+ states observed in this manner in more than twenty targets from Ca to Ce constitutes the giant M1 resonance. The strength of the resonance is only ~1/3 of that predicted. Effects of the T=3/2 Δ isobar may be responsible for much of this quenching. However, our finding of similar quenching in purely isoscalar transitions in ^{28}Si indicates the importance of configuration mixing.

I. Introduction

The study of simple states at high excitation, that is, the study of giant resonances, has taught us much about the structure of nuclei. If we think of such a state as a one particle-one hole (1p-1h) configuration, that configuration will be most easily detected if it is conferred on one state or on a group of close-lying states. Even then, it may be lost in a sea of complex (np-nh) states unless a suitably selective probe is used to excite it.

This paper deals with magnetic, or spin, excitations by direct-reaction inelastic scattering of 200 MeV protons in which there is a transfer to the nucleus of one unit of spin angular momentum but of no orbital angular momentum. For an even-even target the transition is $0^+ \rightarrow 1^+$; hence the designation "M1". The small-angle selectivity for ℓ=0 transfers is an essential part of the experimental technique. In this domain the central force part of the effective nucleon-nucleon interaction is dominant, that is, the tensor and $\vec{L}\cdot\vec{S}$ parts can usually be neglected to good approximation. For purposes of discussion, then, it is sufficient to consider only the spin-transfer, V_σ, and the spin-isospin-transfer, $V_{\sigma\tau}$, parts of the force.

* Supported by National Science Foundation under grants PHY-80-17605, INT-81-16064 and INT-82-13242.

The historical motivation for this investigation was the observation[1,2] of the isobaric analog of the 1^+ state in the ^{90}Zr (p,n)^{90}Nb reaction after a search[3] for the parent 1^+ state in the ^{90}Zr(p,p')^{90}Zr reaction at 24 MeV had failed to find any 1^+ states. We now understand on both theoretical[4] and experimental[5] grounds that the energy dependence of the various parts of the effective interaction makes 200 MeV a much better energy than 24 MeV for

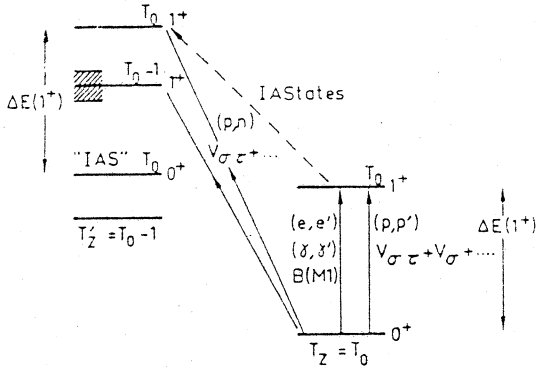

Fig. 1. Relationships between (p,n), (p,p') and electromagnetic interactions for exciting 1^+ states.

seeing 1^+ states amidst a host of natural-parity states. The relevant $0^+ \rightarrow 1^+$ transitions are illustrated by arrows in Fig. 1, and peaks corresponding to transitions to the T_o and T_o-1 1^+ states are indicated in Fig. 2 for Zr(p,n) reactions. Isospin geometry and configuration mixing greatly favor the T_o-1 transition; the T_o peak is weak but present. In ^{90}Nb its energy above the 0^+ isobaric analog of the target ground state is about 8.5 MeV and its fitted width is 1.7 MeV. The 1^+ parent state should exist in ^{90}Zr with similar excitation energy and width.

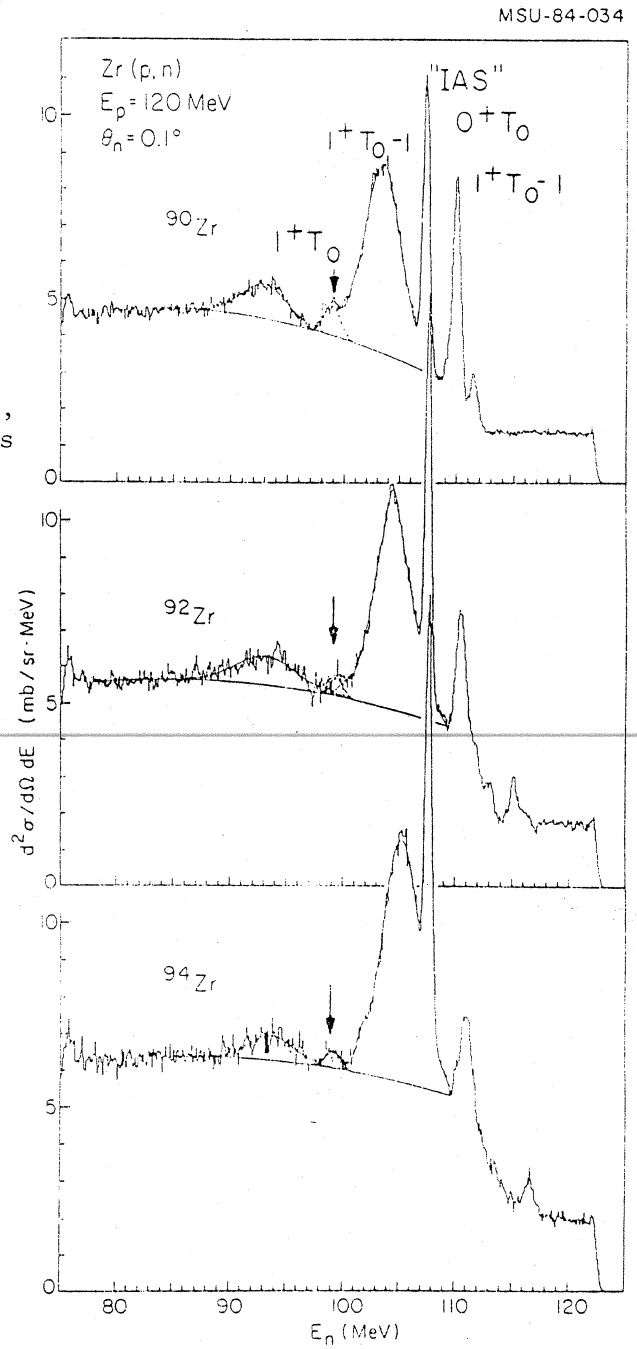

Fig. 2. Neutron spectra at 0.2° for ^{90,92,94}Zr(p,n) at E_p =120 MeV. Note the T_o 1^+ peak in each spectrum at an excitation energy of about 8.5 MeV above the "IAS".

II. The M1 Resonance in Zr Nuclides

The M1 resonance in (p,p') was seen first[6] in ^{90}Zr and then[7] in ^{92}Zr, ^{94}Zr, and ^{96}Zr. Some of the spectra are shown in Fig. 3. An arrowhead marks the centroid of the resonance in each spectrum. In agreement with the expectations from the (p,n) experiments, the centroid in ^{90}Zr is at 8.9 MeV and the width is 1.5 MeV.

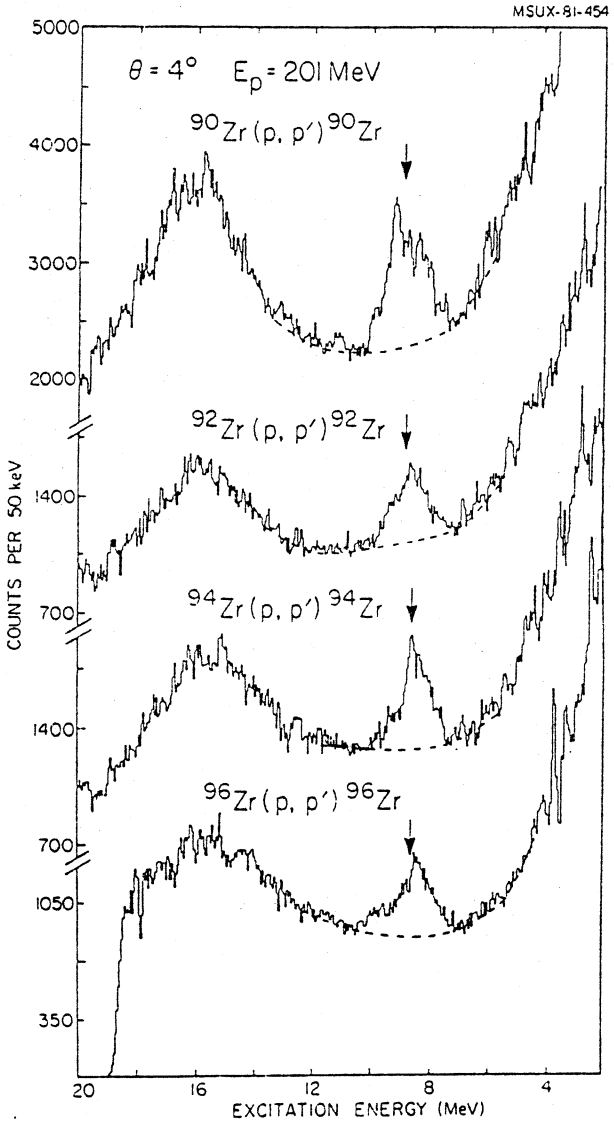

Fig. 3. Spectra of 200 MeV protons inelastically scattered from ^{90}Zr, ^{92}Zr, ^{94}Zr and ^{96}Zr at 4°. The arrows indicate the centroids of the M1 resonance.

The angular distributions are shown in Fig. 4. They are very sharply forward peaked and agree with those predicted by DWBA calculations and with the angular distribution[8] of the (p,n) reaction to the T_o-1 1^+ (giant Gamow-Teller) state measured at 200 MeV. The curves shown in Fig. 4 were computed with the codes DWBA 70[9] and RESEDA[10] using wave functions derived from shell model calculations.[11] Each program uses phase shifts obtained from free nucleon-nucleon scattering, but DWBA 70 requires input in terms of the parameters of an effective interaction. It also results in division of the scattering into direct and exchange parts. The parameterization of Love and Franey[4] was used. If the approximations used in each treatment are good, the results should agree, and as we see in Fig. 4, they are quite similar. For each code the same scaling factor, 0.26, was used to fit the ^{90}Zr data. This number is about the same as the fraction of the predicted B(M1) strength observed in an (e,e')

experiment[12] and about half the quenching factor observed for the Gamow-Teller strength in (p,n) reactions.[1,13]

In ^{90}Zr a bump similar to that shown here was also observed at TRIUMF[14], and in a recent experiment at LAMPF[15] with 319 MeV protons, cross sections, analyzing powers, and spin-flip probabilities were measured. The spin-flip measurements confirm the 1^+ assignment.

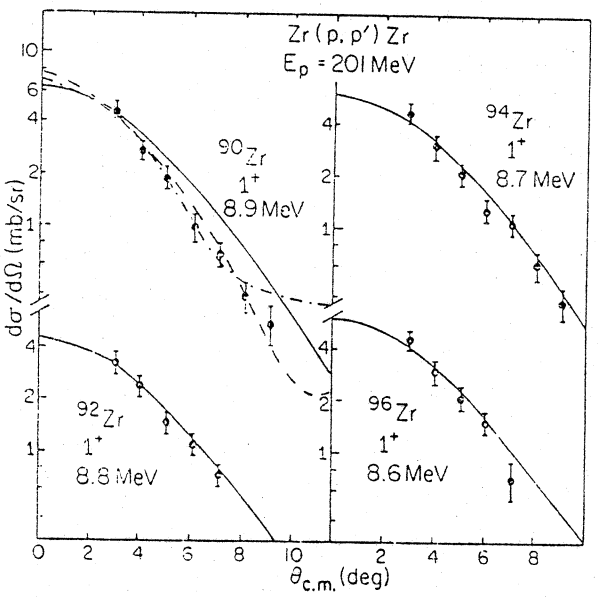

Fig. 4. Angular distributions for the M1 state in ^{90}Zr, ^{92}Zr, ^{94}Zr and ^{96}Zr observed in (p,p') at 200 MeV. The solid curves are DWBA 70 calculations and the dashed curve is a RESEDA calculation. All calculations are normalized to the data at forward angles. The dotted-dashed curve is from a ^{90}Zr(p,n) measurement at 200 MeV.

III. Experimental Equipment--The Orsay Spectrograph System

The work reported here was performed with the 201 MeV proton beam of the Orsay synchrocyclotron and a magnetic spectrograph whose focal plane detection system[16] includes two multi-wire proportional counters and an on-line computer. This system enables one to reduce one of the two sources of background which are important at small angles, namely, protons reaching the focal plane after scattering in slits or the walls of the spectrometer vacuum chamber. Such protons can be identified by the angles at which they cross the focal plane. A spectrum of angles, horizontal or vertical, in Fig. 5 illustrates the procedure. The cross-hatched part corresponds to the scattered protons. By selecting only angles between the two indicated vertical lines, the signal-to-noise ratio is enhanced. The selection is a software selection; it can easily be changed by a re-play of the stored events.

Most of the protons in the beam are contained within an energy band of a few hundred keV and are dispersion matched to the spectrometer at the target. A small number, however, have lower energies. Via elastic scattering they constitute the other background which is important at small angles. Improvements in the technique of transporting the beam from the cyclotron to the target have significantly reduced this background. For example, the ^{90}Zr spectrum in Fig. 6, a spectrum obtained in 1983, has less than half the background of the 1981 ^{90}Zr spectrum of Fig. 3.

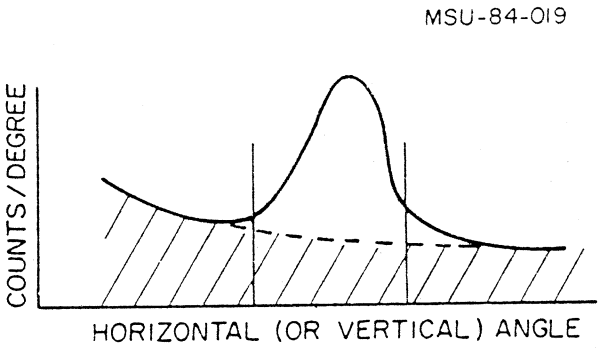

Fig. 5. Trajectory mapping in the focal plane detection system of the Orsay spectrograph. By setting a software window around the peak, the background (cross-hatched) can be reduced.

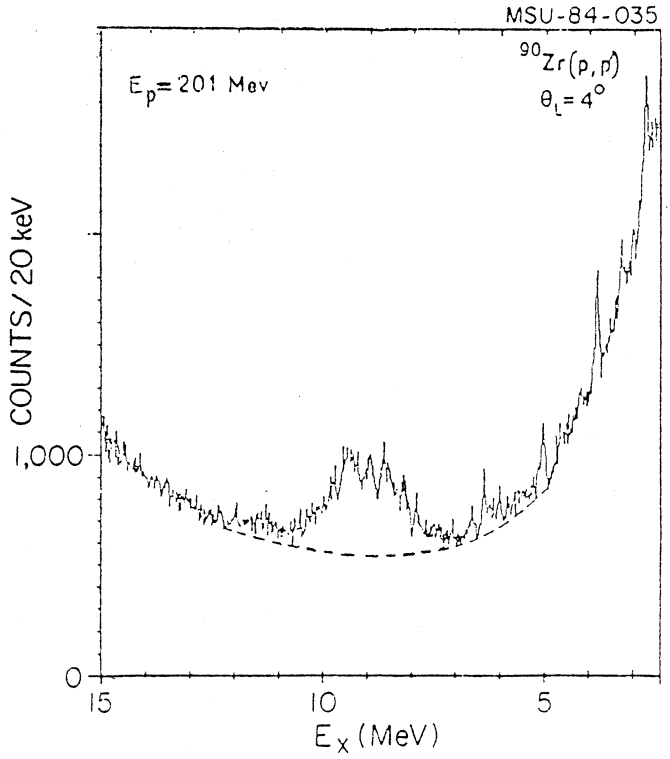

Fig. 6. Spectrum of ^{90}Zr(p,p') taken with improved beam transport resulting in lower background. Compare with ^{90}Zr spectrum in Fig. 3.

As do other multi-wire counters, ours exhibit a degree of differential non-linearity. An obvious example is the dip around 18 MeV in the ^{96}Zr spectrum of Fig. 3. To distinguish the spurious from the real, we always measure a spectrum twice, each time with a different magnetic field. When plotted as a function of energy rather than position a spurious peak will shift a predictable amount; a real peak will repeat in place. This procedure is not foolproof, especially for weak peaks, and it is a bit cumbersome. It is better to also measure and correct for the response of the detector. A spectrum which is already known and which is

smooth and flat makes a good reference spectrum. Such a spectrum, as determined[17] with Ge detectors, is obtained around 100 MeV excitation energy in Pb(p,p') at 200 MeV. This is the "actual" spectrum sketched in Fig. 7; the "measured" spectrum reveals the counter defects. The response function is the

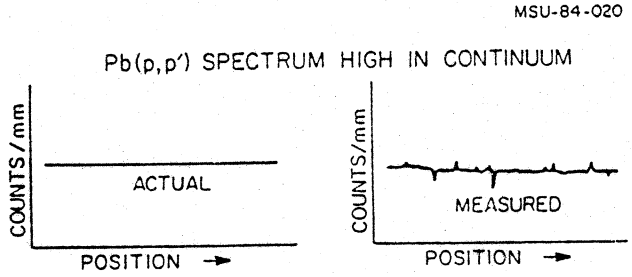

Fig. 7. Schematic focal-plane spectra used to determine detector response and correct for non-linearities.

"measured" divided by the "actual" or, equivalently, by a smooth fit to the "measured". To correct a spectrum for the non-linear defects we perform a channel-by-channel division of the spectrum by the response function. The correction is, of course, only as good as the statistical accuracy, usually 2-3%, with which the Pb spectrum is measured.

IV. M1 Resonance in Various Targets

By this time we have searched for ℓ=0, spin-flip strength via (p,p') in 29 nuclei from ^{24}Mg to ^{208}Pb. Some of the spectra for Mo isotopes are shown in Fig. 8, for ^{51}V in Fig. 9, and for other N=28 nuclei in Fig. 10.

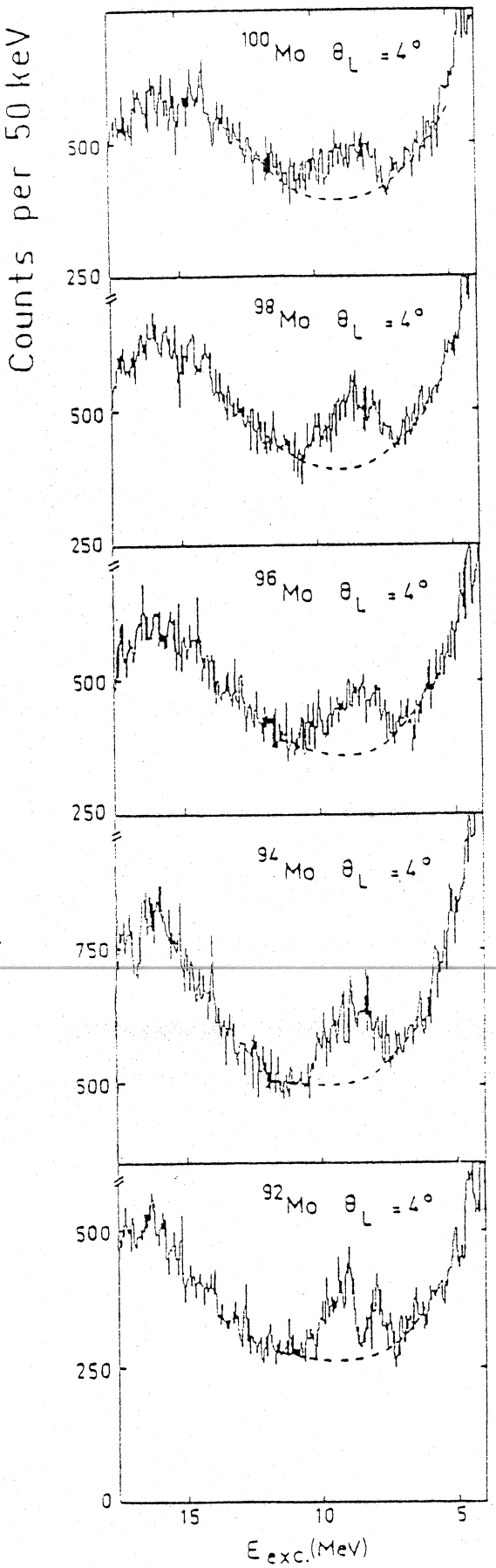

Fig. 8. Spectra of 200 MeV protons inelastically scattered from ^{92}Mo, ^{94}Mo, ^{96}Mo, ^{98}Mo and ^{100}Mo at 4°.

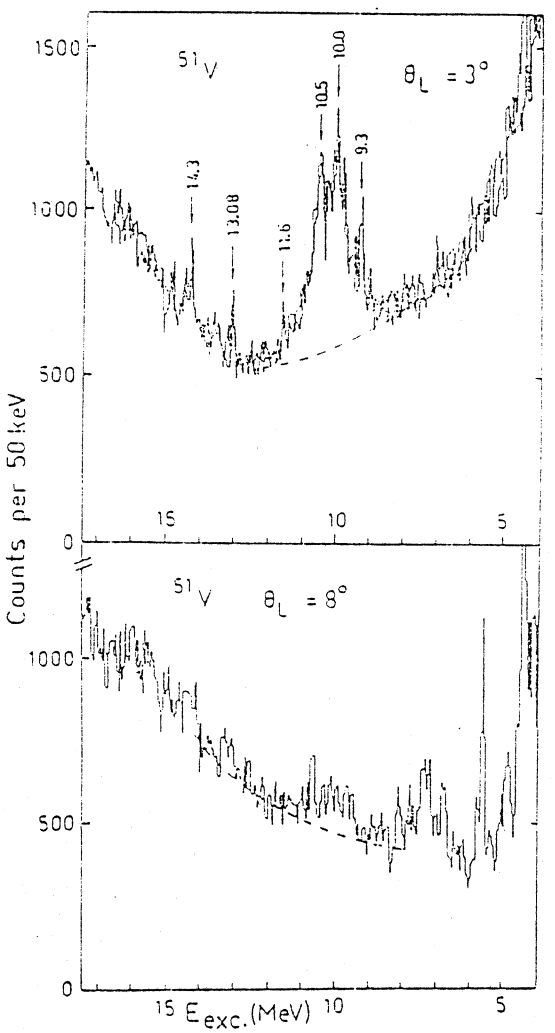

Fig. 9. Spectra of 200 MeV protons inelastically scattered from ^{51}V and 3° and 8°. At 3° the overlap of two spectra taken with different magnetic fields is shown.

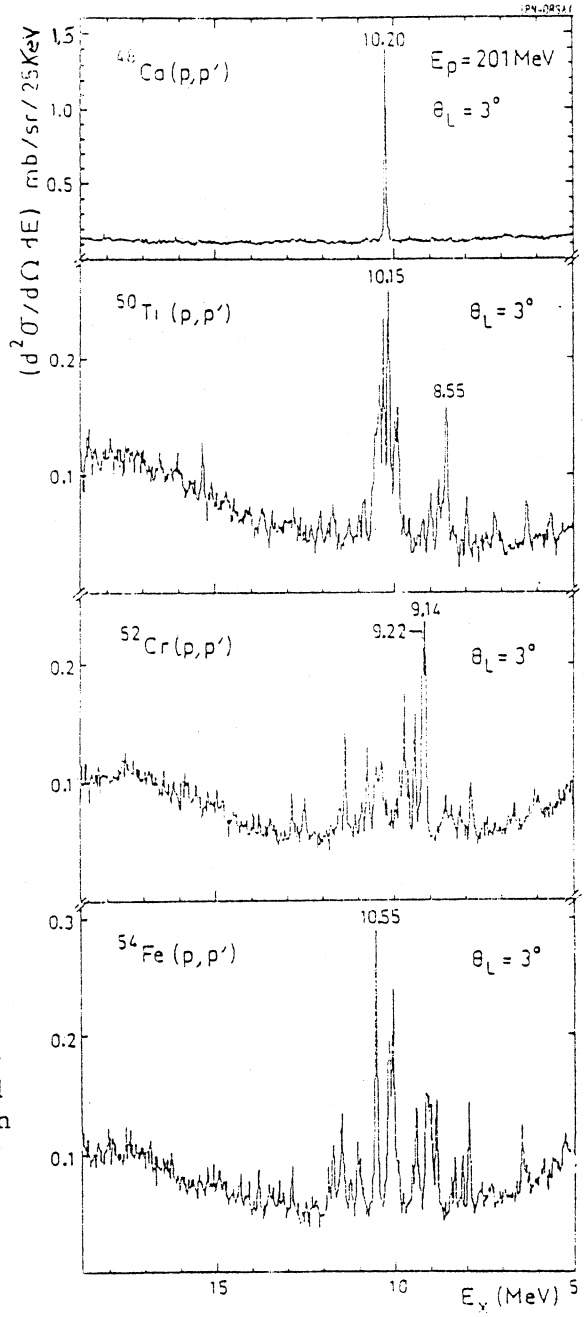

Fig. 10. Spectra of 200 MeV protons inelastically scattered from ^{48}Ca, ^{50}Ti, ^{52}Cr, and ^{54}Fe at 3°.

Each Mo spectrum is broad and structured, as in the Zr spectra. In all cases either a broad feature or individual levels were observed to have very peaked angular distributions.

The sharpness of the angular distribution typical of all M1 peaks is demonstrated in Fig. 9 which shows two spectra from ^{51}V. The prominent peak seen clearly at 3° has practically disappeared by 8°.

Nearly all the states in Fig. 10 between 8 and 15 MeV excitation energy have a forward peaked angular distribution well fitted by an ℓ=0 shape. As one adds protons to ^{48}Ca in moving to ^{54}Fe, the simple state at 10.2 MeV

excitation energy in ^{48}Ca, which presumably arises mainly from neutron excitation with the configuration $\{f_{7/2}^{-1}, f_{5/2}\}^{1+}$, splits up into a number of different states. In ^{50}Ti, this neutron excitation is still visible as a cluster of states whose centroid is very close to the centroid of the simple state in ^{48}Ca. Also visible in ^{50}Ti is a further cluster of states near 8.5 MeV excitation energy. These states are predicted in the model of Metsch and Knupfer[18] to arise mainly from proton excitations with the same configuration $\{f_{7/2}^{-1}, f_{5/2}\}^{1+}$. However, for ^{52}Cr and ^{54}Fe the strength is spread more widely between 8 and 12 MeV excitation energy, and it is no longer possible to devide the states into neutron and proton excitations.

Examples of angular distributions for some individual states in ^{50}Ti are shown in Fig. 11. Within the experimental errors they are all identical. This shape is well reproduced by the angular distribution computed for a strong model state at 13.00 MeV which is excited by a pure isovector interaction. The model[18] might not assign individual strengths correctly, but the summed strength should be more reliable. We see, however, in Fig. 11 that the theory overpredicts by a factor of four -- another example of spin-flip quenching. The quenching factors for ^{52}Cr and ^{54}Fe with the same model are 0.28 and 0.44, respectively. The distribution of 1^+ strength in these four N=28 nuclei as found in our (p,p') data is in general agreement with that obtained from (e,e')[19] and (γ,γ)[20]. For ^{51}V, however, where we observe a strong resonance centered at 10.15 MeV (Fig. 9), no M1 transitions at all are seen in (e,e')[21]. The frequent agreement between (p,p') and (e,e') is not

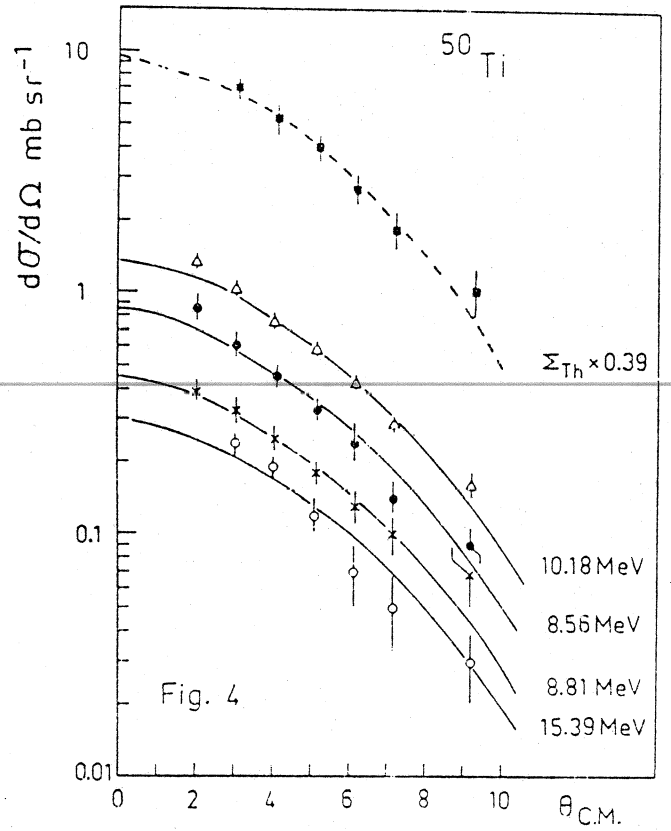

Fig. 11. Angular distributions for some representative 1^+ states excited in ^{50}Ti(p,p') at 200 MeV. See Fig. 10. At the top is the angular distribution for the sum of all the 1^+ states observed and a theoretical curve (see Ref. 18) scaled by the factor 0.39 to fit the data.

surprising, since spin-flip is often the dominant mechanism of both reactions. When proton excitation is part of the M1 transition, however, there can be cancellation between the orbital and spin parts of the B(M1) amplitude. One can wonder if a detailed calculation would show extreme cancellation when there are three $f_{7/2}$ protons but not when there are two, four, or six $f_{7/2}$ protons.

In our survey of the M1 resonance through a part of the periodic table, A=40 to 140, our primary experimental signature of a $0^+ \rightarrow 1^+$ transition has been an $\ell=0$, forward-peaked angular distribution. We rule out $0^+ \rightarrow 0^+$, because that is a natural-parity transition which should be more strongly excited at commonly used lower energies than at 200 MeV. Also, sometimes (α,α') has been done; non-observation of a state is then consistent with that state being 1^+. Unfortunately, an electric dipole transition, $0^+ \rightarrow 1^-$, excited through the Coulomb interaction, also produces a forward-peaked angular distribution. In fact, its distribution is more sharply peaked in medium-mass nuclei than is an $\ell=0$ transition, and one can choose between 1^+ and 1^- on that basis. In heavy nuclei Coulomb excitation is very strong, and the 1^+ and 1^- angular distributions are very similar. In ^{208}Pb, Fig. 12, most of the strongly-excited states are 1^- states, and we have found very little 1^+ strength.

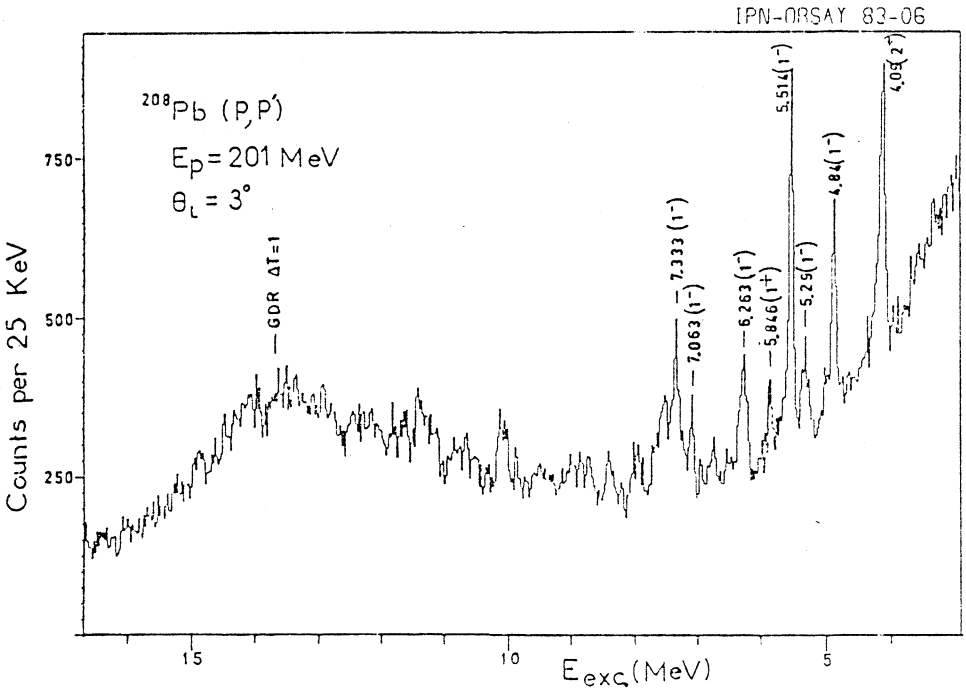

Fig. 12. Spectrum of protons at 3° from ^{208}Pb(p,p') at 201 MeV. Most of the large peaks are 1^- states excited by the Coulomb interaction.

The excitation energies of the centroids of the 1^+ structures found between A=40 and 140 are plotted in Fig. 13. There is only a slow fall-off from about 10 to 8 MeV. The M1 excitation energy depends upon the spin-orbit splitting and a

residual particle-hole interaction. As A increases and the effect of a finite nucleus diminishes, the spin-orbit energy decreases for a given ℓ-value. Of course, the relevant ℓ-value increases with A, and so the two factors run counter to each other. Thus, one can qualitatively understand the observed behavior. A more quantitative calculation[23] matches the data quite well.

When we have had wave functions or when we assumed simple wave functions and computed an expected differential cross section, the angular dependence was correct, but the magnitude was too large. The ratio of experiment to theory, i.e., the quenching factor Q, is given in Table I. below.

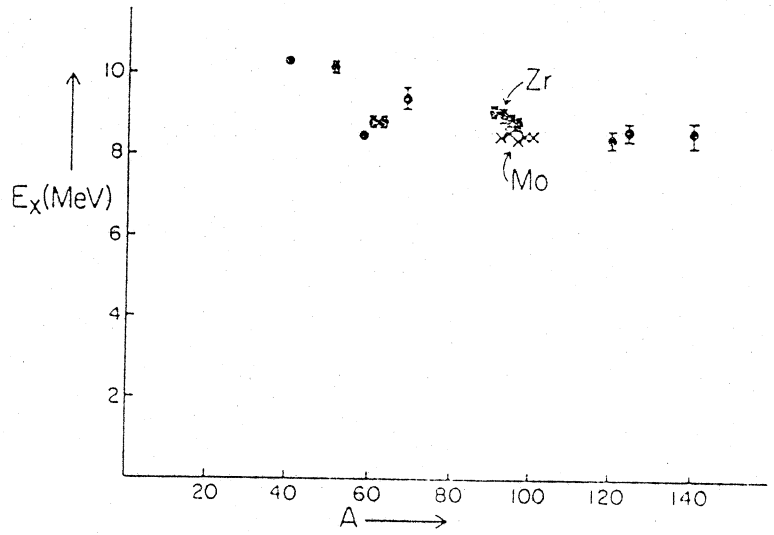

Fig. 13. Target mass dependence of the excitation energy of the giant M1 resonance observed in the (p,p') reaction at E_p=200 MeV.

Table I: Quenching factors obtained in 200 MeV (p,p') excitation of the giant M1 resonance.

Nucleus:	^{50}Ti	^{52}Cr	^{54}Fe	^{58}Ni	^{90}Zr	^{92}Mo	^{120}Sn	^{140}Ce
Q :	0.39	0.36	0.35	0.23	0.26	0.34	0.27	0.25

The calculations were all done using the code RESEDA with the Paris potential. Q appears to be almost constant with mass number.

V. The Ideal Case - ^{48}Ca

The consistency of the quenching reported above may be taken as some measure of its correctness. However, simplifications have, of necessity, been made in the wave functions, and, from looking at the spectra one gets the feeling that some of the M1 strength may not be identifiable. If the M1

resonance were excited by a single spin-orbit pair (i.e., one ℓ-value), and if the excitation were very concentrated in energy, we would have an ideal case to see if there was really less cross section than predicted. An experiment[24] at Darmstadt showed that ^{48}Ca may provide that case. The (p,p') spectrum for ^{48}Ca is a very dramatic one. Indeed, in no other target hve we seen such an extreme concentration of ℓ=0, spin-flip strength. As shown in Fig. 14, this concentration allows a beautiful demonstration of the ℓ=0 selectivity at small angles. The sharpness of the peak leaves little ambiguity in the background subtraction. Hence, the cross section can be obtained quite accurately. Also, one expects that the closed-shell approximation for the ground state of ^{48}Ca is rather good, and, furthermore, a complete f-p shell basis has been used[25] to generate more accurate wave functions.

Microscopic distorted wave calculations have been carried out using the codes RESEDA and DWBA 70. The 10.2 MeV data and the computed differential cross sections are given in Fig. 15. Two of the curves were computed assuming a closed shell (simple W-F) and one with the eight excess neutrons assumed not so restricted (full W-F)[25]. Details of the calculations have

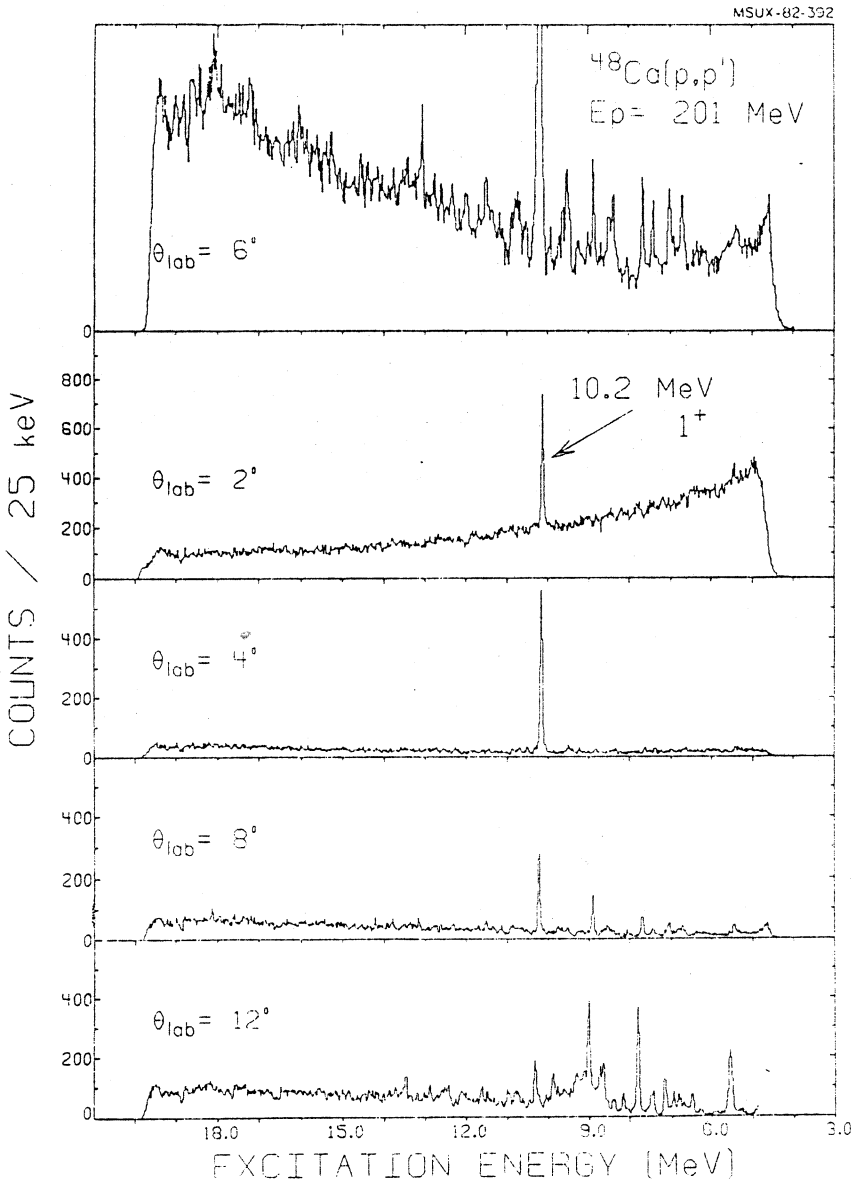

Fig. 14. Spectra of protons inelastically scattered from ^{48}Ca at angles from 2° to 12°. The uppermost spectrum has been scaled to show the weakly excited states.

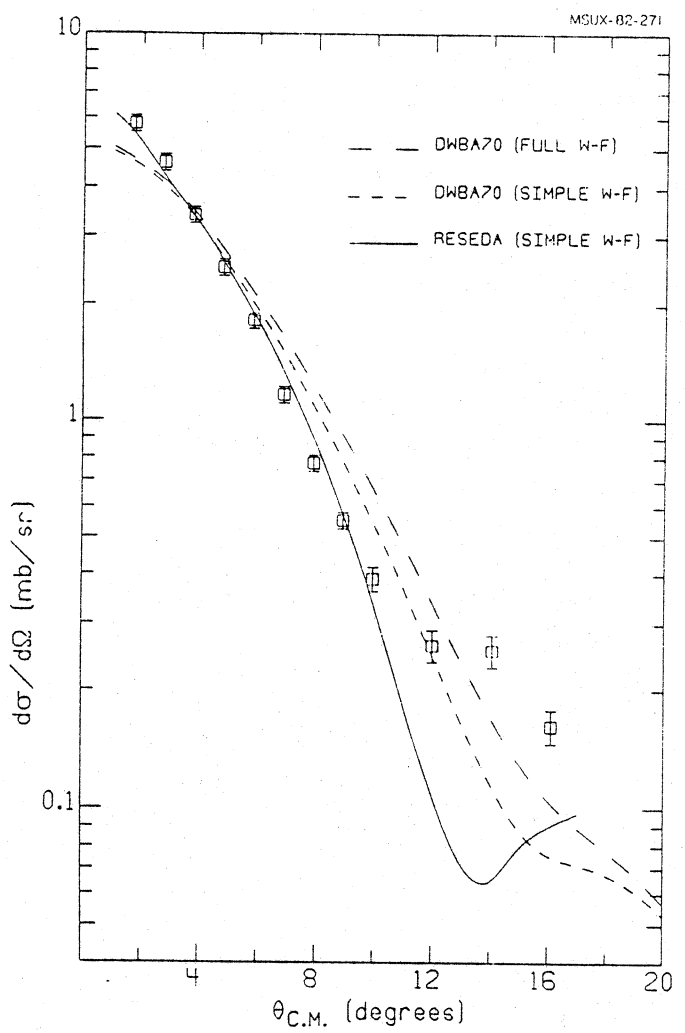

Fig. 15. Angular distribution for $^{48}Ca(p,p')$ to the 10.2 MeV state. The points are the measured values and the curves are from calculations described in the text.

been given in a recent publication[26]. The main result is that the simple W-F gives Q = 0.24 with RESEDA and Q = 0.21 with DWBA 70, and the full W-F gives Q = 0.30. (With a modified effective interaction[27] Q = 0.33.) So, the quenching in this ideal case is about the same (See Table I.) as in the more complex cases.

Since we are dealing with an excitation which is almost a pure neutron excitation, quenching should appear in (p,p'), (p,n)[28] and (e,e')[19] reactions in comparable proportions. Only the sharp peak at 10.2 MeV is observed consistently in the different reactions. The quenching factors for excitation of this state are given in Table II. The (p,p') values are the lowest, but they are indeed comparable to the other two.

Table II: Quenching factors for excitation of the 10.2 MeV state of ^{48}Ca.[a]

	(p,p')	(p,n)	(e,e')
Closed-shell wave function	0.22	0.26	0.33
Full f-p shell wave function[b]	0.30 (0.33)	0.35	0.47

a) See Ref. 26 for more details.
b) Ref. 25

As is evident in Fig. 14, other states are excited at the larger angles. In runs with better statistics than those in Fig. 14 many of these states could be tracked down to 3°. The differential cross sections for five of them (plus the 10.2 MeV state for reference) are given in Fig. 16. At least two of them, the states at 12.14 and 10.76 MeV, have forward peaking similar to that of the 10.2 MeV state. The fact that the fall-off does not persist with angle is probably caused by unresolved states excited with ℓ-values >0. (The instrumental resolution is 60-70 keV). If we count all such forward peaking as indications of 1^+ states, the total observed M1 strength is increased by one-third. A quenching factor of 0.3 for the 10.2 MeV state grows to 0.4 when these small components are included. It is still possible that there is significant additional M1 strength too finely distributed to be detected with the present resolution.

VI. Quenching in Isovector and Isoscalar Transitions

Since $V_{\sigma\tau}$ is much larger than V_{σ} at 200 MeV, the M1 transitions are predominantely isovector transitions, and the quenching we have discussed is predominantly isovector quenching. The only way to observe isoscalar transitions in (p,p') reactions is to use a T=0 target. Then transitions to T=0 excited states will be purely isoscalar and transitions to T=1 excited states will be purely isovector. The familiar Δ isobar explanation[29] of M1 and Gamow-Teller quenching is not a possible explanation of isoscalar

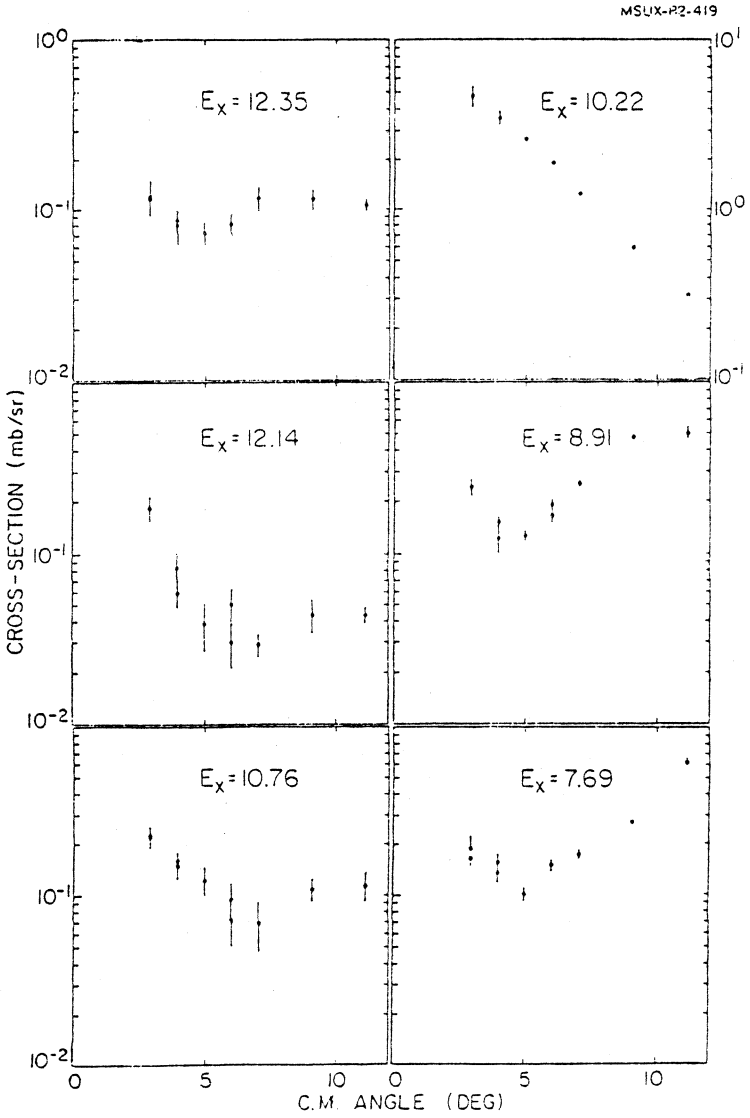

Fig. 16. Angular distributions of some of the weakly excited states (see top Fig. 14) in $^{48}Ca(p,p')$. The strong state at 10.2 MeV is included for comparison.

quenching, except for small second-order effects. Only configuration mixing can produce sizeable isoscalar quenching, whereas both mechanisms are active in isovector quenching. Hence, a study of isoscalar spin-flip quenching could shed light on the origin of both isoscalar and isovector quenching.

For this purpose we have selected several T=0 targets in the s-d shell and have analyzed the data for ^{28}Si. A spectrum is shown in Fig. 17. The peaks with arrows above them are T-1, 1^+ states; the peak at 9.50 MeV is a T=0, 1^+ state.

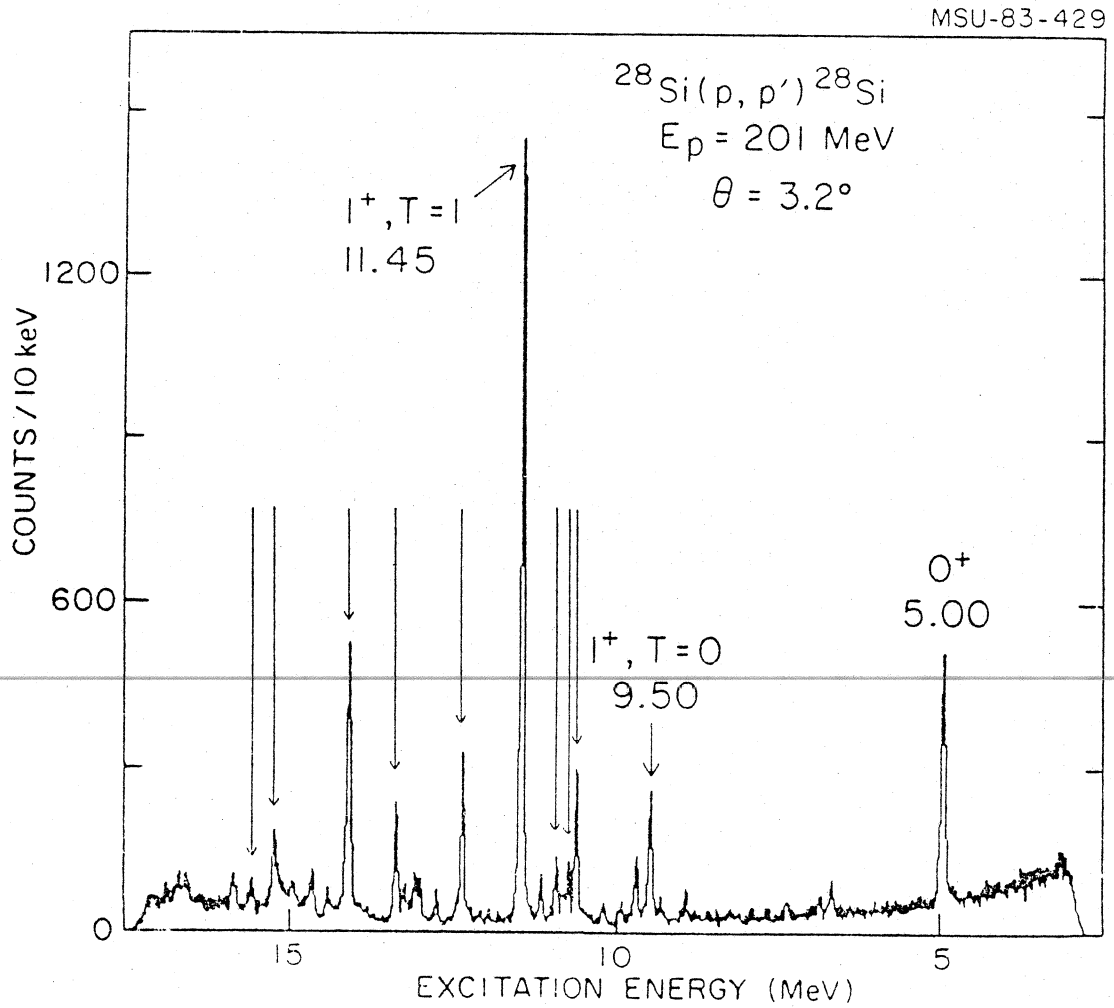

Fig. 17. Inelastic proton spectrum for ^{28}Si at 3.2°. The arrows indicate the one T=0 and the nine T=1 1^+ states observed.

Angular distributions for six of the nine observed T=1 states and for the T=0 state are shown in Fig. 18. The curves were computed with the code DWBA 70 in the usual manner. Fortunately, we were able to use wave functions[30] in which the twelve nucleons outside of a ^{16}O core were unrestricted in the s-d shell. Hence, a good deal of configuration mixing is already included in the theoretical cross sections. The angular distribution for the T=0 state (E_x=9.50 MeV) is much flatter than the angular distributions observed for the

T=1 1^+ transitions. The DWIA calculations reproduce both the T=0 and T=1 data. The difference in the shapes can be understood qualitatively as being ue to the strong, attractive $V_{0\tau}$ interaction present only in the T=1 channel. The good fit obtained for the angular distribution of the 9.50 MeV state is an indication of the pure isoscalar nature of this state. (A known 2^+ level at 9.48 MeV is unresolved from the 9.50 MeV level. Its shape is that which we measured for a known 2^+ doublet at 7.38-7.42 MeV, while its magnitude has been arbitrarily adjusted.)

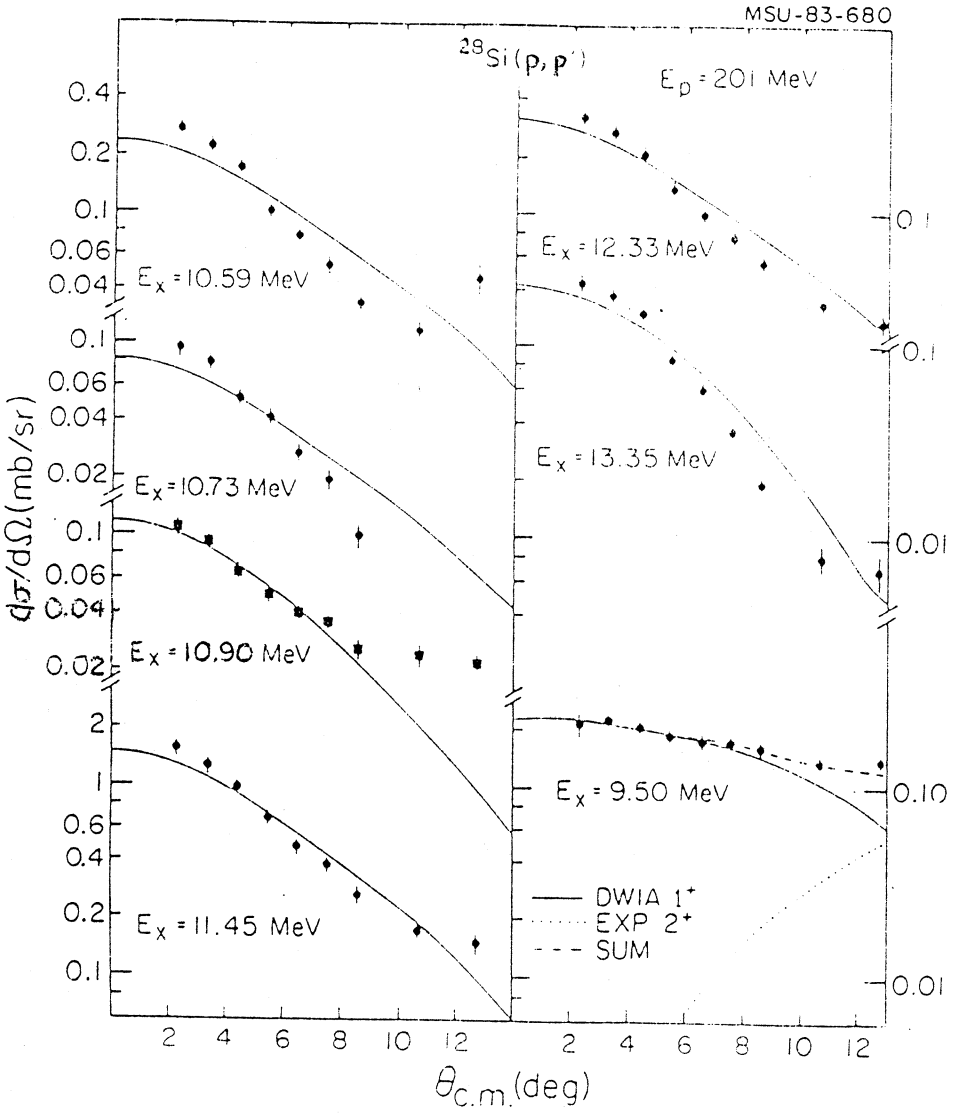

Fig. 18. Angular distributions for seven 1^+ states, one (at E_x = 9.50 MeV) with T=0 and the others with T=1. The solid curves are the results of DWIA calculations discussed in the text. The dotted curve for the 9.50-MeV doublet represents the experimental shape for a 2^+ state and the dashed line is the sum of the solid and dotted curves.

4) W.G. Love and M.A. Franey, Phys. Rev. C 24, 1073 (1981).

5) T.N. Taddeucci et al., Phys. Rev. C 25 1094 (1982).

6) N. Anantaraman et al., Phys. Rev. Lett. 46, 1318 (1981).

7) G.M. Crawley et al., Phys. Rev. C 26, 87 (1982).

8) C. Gaarde et al., Nucl. Phys. A369, 258 (1981).

9) J. Raynal and R. Schaeffer, CEN, Saclay report, unpublished (1970).

10) A. Willis, Ph.D. Thesis, University of Paris, unpublished (1968).

11) C. Djalali et al., Nucl. Phys. A388, 1 (1982).

12) D. Meuer et al., Nucl. Phys. A349, 309 (1980).

13) C. Gaarde, J.S. Larsen and J. Rapaport, Proc. Tellwide Conf. on Spin Excitations in Nuclei (1982).

14) F.E. Bertrand et al., Phys. Lett. 103B, 326 (1981).

15) S.K. Nanda et al., Phys. Rev. Lett 51, 1526 (1983).

16) A. Willis et al., Nucl. Phys. A344, 137 (1980) and c. Djalali, N. Marty, M. Morlet and A. Willis, Nucl. Phys. A380, 42 (1982).

17) J.P. Didelez, Orsay, private communication.

18) B.C. Metsch and W. Knupfer, private communication.

19) G. Eulenberg et al., Phys. Lett. 116B, 113 (1982) and private communications from W. Steffen and A. Richter.

20) U.E.P. Berg et al., Phys. Lett. 103B, 301 (1981) and Nucl. Phys. A398, 397 (1983).

21) D. Bender et al., Nucl. Phys. A398, 408 (1983).

22) C. Djalali et al., Z. Physik A298, 79 (1980).

23) G.F. Bertsch, Nucl. Phys. A354, 157 (1981).

24) W. Steffen et al., Phys. Lett. 95B, 23 (1980).

25) J.B. McGrory and B.H. Wildenthal, Phys. Lett. 103B, 173 (1981).

26) G.M. Crawley et al., Phys. Lett. 127B, 322 (1983).

27) W.G. Love and M.A. Franey, private communication (1982).

28) F. Osterfeld et al., Phys. Rev. Lett. 49, 11 (1982).

29) M. Ericson, A. Figureau and c. Thevenet, Phys. Lett. 45B, 19 (1973); E. Oset and M. Rho, Phys. Rev. Lett. 42, 47 (1979); H. Toki and W. Weise, Phys. Lett. 97B, 12 (1980); A. Bohr and B.r. Mottelson, Phys. Lett. 100B, 10 (1981).

30) B.H. Wildenthal, in "Progress in Particle and Nuclear Physics", Vol. 11, (Pergamon Press), to be published and elsewhere in these proceedings.